The Journal of the Oceanological Society of Korea
Vol. 15, No. 1, p. 1-7, June 1980

WAVE GENERATION AND WIND-INDUCED SHEAR CURRENT IN WATER

Injune Choi

Korea Ocean Research and Development Institute, KIST

ABSTRACT

The results of measurements of shear current induced in water by wind in wind wave tunnel are presented briefly. The shear current distributions are found to fit reasonably well an exponential form. This form was used to estimate surface velocity and boundary layer thickness used in stability analysis. An analysis of hydrodynamic stability of the shear current was carried out, using a broken line as an approximate profile, to see the stability as a possible mechanism of wind wave generation. Comparison between experimental results and theoretical ones shows that there exists a large discrepancy particularly in phase velocity and hydrodynamic instability of the shear current seems not to be the basic mechanism of wind wave generation.

INTRODUCTION

When wind blows over a calm surface of water at rest, the first phenomenon we observe is a strong shear current which is followed by the formation of waves. The shear current is induced near air-water interface by a tangential stress acting at the interface. In the wind-wave tunnel where the fetch is limited, a moderate wind produces three distinguishable water surface zone at the lower fetch values: A relatively smooth zone, with no visible or measurable wave motion, but with very rapid drift current development; The preceding smooth zone is followed by a second domain where first visible waves are generated inside divergent streaks. Their motion is almost two dimensional; Finally the streaks meet each other and the wave motion becomes apparently random and three dimensional.

Although during recent decades many attempts (e.g., Miles (1957); Phillips (1957)) have been made to understand the phenomenon of wave generation by wind, the physical mechanism concerned is not considered as known satisfactorily. Most of the work searching for the origin of the wave is based largely on two basic ideas: Resonance mechanism between the turbulent fluctuation of pressure in the air and the calm water surface; Hydrodynamic instability mechanism of either air flow only or combined flow of air and water.

Based on the idea that the wave generation may be associated with hydrodynamic instability of the shear current induced in water by wind, Stern and Adam (1973) carried out a rough instability analysis of the shear current.

In this paper first we will present briefly the results of shear current measurements in a wind-wave tunnel in the first zone described above where we observe no measurable wave motion. Then we consider analytically the hydrodynamic stability of that flow field as a possible mechanism of wind wave generation using a broken line approximation to the shear current. Then we will compare these analytical results with measurements.

LABORATORY EXPERIMENTS

1. Experimental Conditions.

The measurement was performed in the wind-wave facility at the Institut de Mécanique Statistique de la Turbulence, Marseille, France. This facility is described in detail by Coantic and Favre (1970). Briefly the facility has a surface of water of 0.52m wide and 8.65m long. Its depth is about 0.26m maintained constant by a small water pump. The schematic representation of the physical situation is shown in Figure 1. The air flow in the entrance of the experimental section is arranged to have a fully developed turbulent boundary layer, its thickness being about 10cm for the wind velocity of U_∞= 5m/s. The wind velocity was chosen as 5m/s so that we can have three zone, described in the introduction, extended over a large fetch length. The phase velocity and the dominant frequency of the first wave appearing in the second zone are 29cm/s and 16 Hz respectivly with wave number $k=3.65cm^{-1}$, wave length 1.81cm and wave amplitude 0.7mm.

The water velocity profile was measured by a conical type hot film anemometer using the anemometry channel manufactured by DISA Elektronik A/S, working at a constant temperature mode. It is well known that this sensor is particulary adapted to the study of water flow. The range of the velocity which interests us is of the order of 20cm/s or less.

2. Shear Current Profile.

For obvious reasons, measurements were limited to the first zone where no wave motion was present. Shear current was measured as a function of depth y at four different stations; x=1.5cm, 15.5cm, 32.5cm and 46cm to see the development as a function of fetch. In Figure 2, the velocity profile is plotted on a linear-linear scale. It is important to note that at each station the point represented in Figure 2 is the result of several independent measurements, which means that the phenomenon may be repeated with great precision.

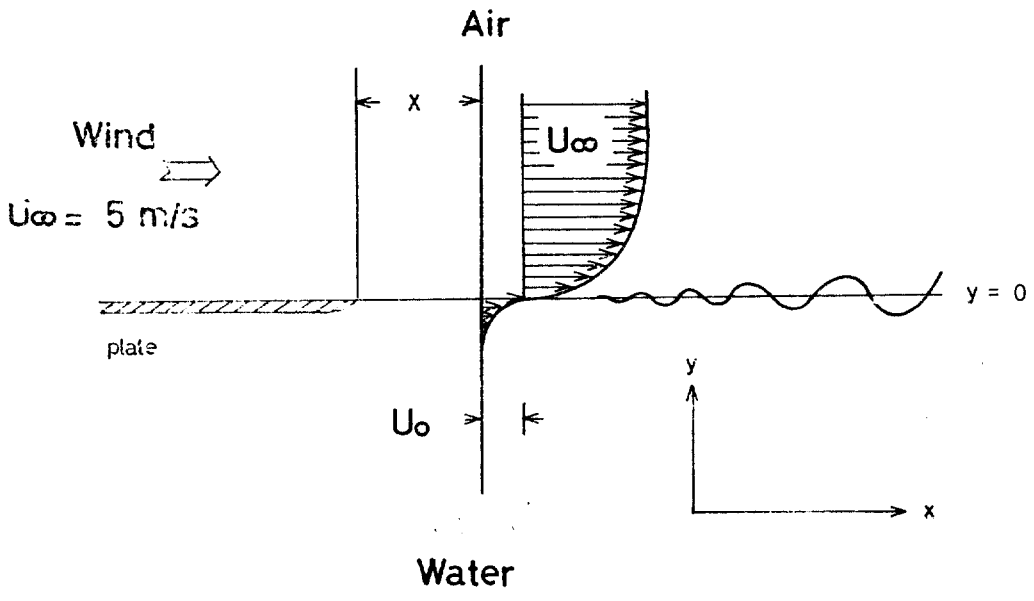

Fig. 1. Schematic representation of the physical situation.

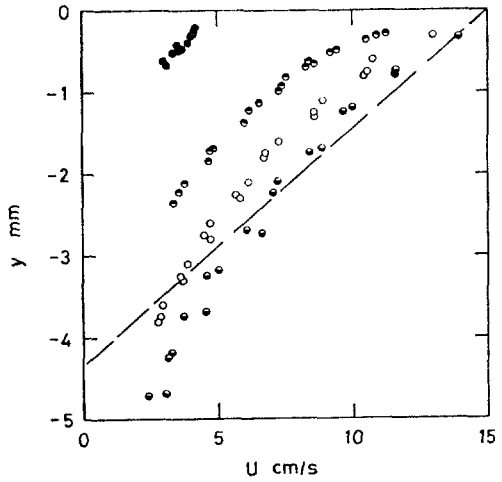

Fig. 2. Shear current distribution as a function of fetch (χ) and depth (y) and broken line profile used in analysis. ●, χ=1.5cm: ◓, χ=15.5cm; ○, χ=32.5cm; ◒, χ=46cm.

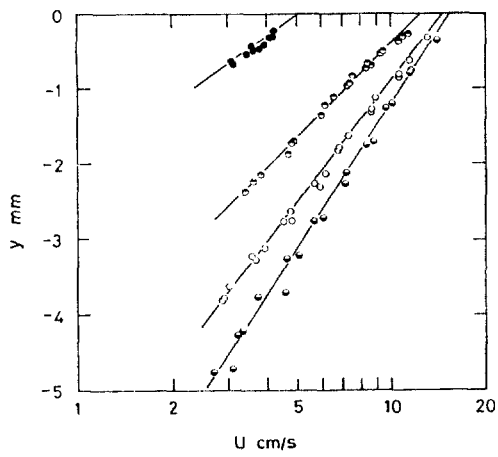

Fig. 3. Shear current distribution fitted to the exponential form as a function of fetch and depth. ●, χ=1.5cm; ◓, χ=15.5cm; ○, χ=32.5cm; ◒, χ=46cm.

To estimate the surface velocity and boundary layer thickness for the discussion of analytical results, we try to fit the measured points to the following exponential form which is chosen by several authors, particularly by McLeish et al (1975).

$$U(y) = U_o e^{by}$$

where U_o: surface velocity

b: constant characterizing boundary layer thickness

The values of U_o and b for different fetch values are estimated from measurements and given in Table 1.

In figure 3, a log-linear plot was used, showing that an exponential change of the velocity with depth provides a reasonable description.

Note that the surface velocity U_o and boundary layer thickness b^{-1} increase as the fetch increases. Futher increase of fetch values does not seem to increase the surface velocity but the boundary layer thickness is increased. The surface velocity seems to keep an almost constant value of about 3% of wind velocity.

Table 1. The values of U_o and b for different fetch values

χ(cm)	1.5	15.5	32.5	46.0
U_o(cm/s)	5.0	12.22	14.53	15.43
b(cm^{-1})	8.0	5.5	4.3	3.6

STABILITY ANALYSIS

1. Governing Equations.

Result of measurements of shear current shows that as fetch increases, the surface velocity increases very rapidly to attain its maximum value while boundary layer thickness increases gradually. Under the assumption that x-variation of shear current profile is small, the shear current profile is taken as $U(y)$ which is independent of x. We also assume that the wave motion is two dimensional and the wind direction is in the positive x direction with positive y normal to it and vertically upwards (Figure 1). The fluid is assumed incompressible and inviscid. The equations governing sufficiently small perturbations of a two-dimensional flow can be obtained by traditional linearization scheme in hydrodynamic stability problem:

$$\frac{\partial u}{\partial x}+\frac{\partial v}{\partial y}=0 \tag{1}$$

$$\frac{\partial u}{\partial t}+U\frac{\partial u}{\partial x}+v\frac{\partial U}{\partial y}=-\frac{1}{\rho}\frac{\partial p}{\partial x} \tag{2}$$

$$\frac{\partial v}{\partial t}+U\frac{\partial v}{\partial x}=-\frac{1}{\rho}\frac{\partial p}{\partial y} \tag{3}$$

with undisturbed state solution

$$P=-\rho g y+P_o \tag{4}$$

where p, u and v are the perturbed part of pressure, x and y component of the velocity respectively and P_o the pressure at $y=0$, ρ the fluid density and g is gravitational acceleration.

Equation (1) permits the use of stream function Ψ where

$$u=\frac{\partial \Psi}{\partial y} \text{ and } v=-\frac{\partial \Psi}{\partial x} \tag{5}$$

We also assume

$$(p,\Psi)=(\hat{p},\hat{\Psi})\ e^{ik(x-ct)} \tag{6}$$

where k is a wave number and c is a complex phase velocity. p and Ψ depend only on y. The displacement of the surface is taken to be

$$\eta=\hat{\eta}e^{ik(x-ct)} \tag{7}$$

where $\hat{\eta}$ is the amplitude.

After eliminating p in equations (2) and (3) and using equations (5) and (6), we can get an equation known as Rayleigh equation

$$(U-c)(\hat{\Psi}''-k^2\hat{\Psi})-U''\hat{\Psi}=0 \tag{8}$$

with

$$\frac{\hat{p}}{\rho}=(c-U)\hat{\Psi}'+U'\hat{\Psi} \tag{9}$$

where $'$ denotes the derivative with respect to y. If we know the form of $U(y)$ and the boundary conditions, we can obtain an eigenvalue equation determining c.

As a first approximation to the shear current profile $U(y)$, we consider the broken line (Figure 2) for mathematical simplicity in the following analysis:

$$\begin{aligned} U(y)&=\frac{U}{d}(y+d) && -d<y\leq 0\\ &=0 && -\infty<y\leq -d \end{aligned} \tag{10}$$

Where U_o is the surface velocity and d is the characteristic boundary layer thickness. Then the equation (8) becomes

$$\hat{\Psi}''-k^2\hat{\Psi}=0 \tag{11}$$

for the layer above and below $y=-d$.

The solution of the equation (11) can be written as

$$\begin{aligned} \hat{\Psi}(y)&=Ae^{ky}+Be^{-ky} && -d<y\leq 0\\ &=Ce^{ky}+De^{-ky} && -\infty<y\leq -d \end{aligned} \tag{12}$$

where A, B, C and D are the undetermined coefficients. With appropriate boundary conditions we can obtain an equation determining c, similar to that given by Stern and Adam (1973).

2. Boundary Conditions and Eigenvalue Equation.

For simplicity we will use the following notation.

$$[G]y=G(y+)-G(y-)$$

for an arbitrary physical quantity G.

As the perturbation must vanish as $y\to-\infty$, we get $D=0$ in equation (12). At the interface the vertical velocity satisfies the kinematic condition

$$\frac{\partial \eta}{\partial t}+U_o\frac{\partial \eta}{\partial x}=v$$

which becomes

$$(U_o-c)\hat{\eta}=-\hat{\Psi} \tag{13}$$

and the condition that the normal stress vanish at the free surface is

$$P+p=-T\frac{\partial^2\eta}{\partial x^2} \qquad \text{at } y=\eta$$

where T is the surface tension. Note that the condition is evaluated at $y=\eta$. The change from $y=\eta$ to $y=0$ gives

$$p=\rho g\eta-T\frac{\partial^2\eta}{\partial x^2} \qquad \text{at } y=0$$

by taking into account (4). Thus we obtain

$$\hat{p}=\rho g\hat{\eta}+k^2T\hat{\eta} \tag{14}$$

The first term on the right is the contribution from the undisturbed state due to the displacement η. Introducing (9), (12) and (13) into (14) gives

$$k(U_0-c)(A-B)-(A-B)\frac{U_0}{d}$$
$$=\left(g+k^2\frac{T}{\rho}\right)\frac{A-B}{U_0-c} \qquad (15)$$

Finally at $y=-d$, the pressure and the stream function are continuous

$$[p]_{-d}=0$$
$$[\Psi]_{-d}=0$$

from which we obtain by introducing equations (9) and (12)

$$ck(Ae^{-kd}-Be^{kd})$$
$$=-(Ae^{-kd}+Be^{kd})\frac{U_0}{d}+ckCe^{-kd} \qquad (16)$$
$$Ae^{-kd}+Be^{kd}=Ce^{-kd} \qquad (17)$$

respectively.

By introducing the non-dimensional variables

$$\kappa=kd,\ r=1-\frac{c}{U_0},\ f=\frac{gd}{U_0^2},\ \theta=\frac{T}{\rho g d^2}$$

and

$$l=-f(1+\kappa^2\theta)$$

the equations (15), (16) and (17) become

$$A(r^2\kappa-r+l)-B(r^2\kappa+r+l)=0$$
$$A[(1-r)\kappa+1]-B[(1-r)\kappa-1]e^{2\kappa}-C(1-r)=0$$
$$A+Be^{2\kappa}-C=0$$

Therefore, these equations in the coefficients A, B and C have nontrivial solutions if and only if the following determinant is zero.

$$\begin{vmatrix} (r^2\kappa-r+l) & -(r^2\kappa+r+l) & 0 \\ (1-r)\kappa+1 & -[(1-r)\kappa-1]e^{2\kappa} & (r-1) \\ 1 & e^{2\kappa} & -1 \end{vmatrix}=0 \qquad (18)$$

from which we can obtain the complex phase velocity as a function of the parameters characterizing the flow:

$$c=F(U_0, d, g, T, \cdots\cdots)$$

The problem consists of determning the sign of the imaginary part of c.

The equation (18) becomes

$$r^3+A_0r^2+A_1r+A_2=0 \qquad (19)$$

where

$$A_0=-\frac{1}{2\kappa}(2\kappa+1+e^{-2\kappa})$$
$$A_1=\frac{1}{2\kappa^2}(2\kappa l+2\kappa-1-e^{-2\kappa})$$
$$A_2=\frac{1}{2\kappa^2}l(1-2\kappa-e^{-2\kappa})$$

The roots of equation (19) are determined depending on the sign of Δ defined by

$$\Delta=\left(\frac{q_1}{2}\right)^2+\left(\frac{q_2}{3}\right)^3$$

where

$$q_1=\frac{2}{27}A_0^3-\frac{1}{3}A_1A_0+A_2 \text{ and } q_2=A_1-\frac{1}{3}A_0^2$$

If $\Delta<0$, there are three real roots and the flow is stable. While if $\Delta>0$, there is one real root and one complex conjugate and the flow is unstable. The neutral stability curve is defined by $\Delta=0$, which gives f as a function of κ and θ. Figure 4 shows the neutral stability curve, given by f as a function of κ for different value of θ. Any point inside the curve is unstable. Figure 5 shows the phase velocity of the most unstable mode, represented as a function of κ. It is independant of θ.

It should be noticed that for a velocity profile $U(y)$ which decreases monotonically as depth

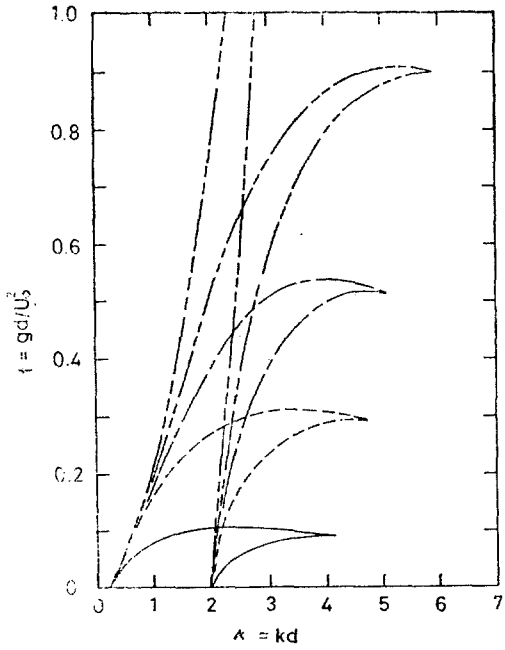

Fig. 4. Neutral stability curves for different values of ——, $\theta=0$; — —, $\theta=0.1$; — —, $\theta=0.2$; — — —, $\theta=0.4$; ——, $\theta=1.5$.

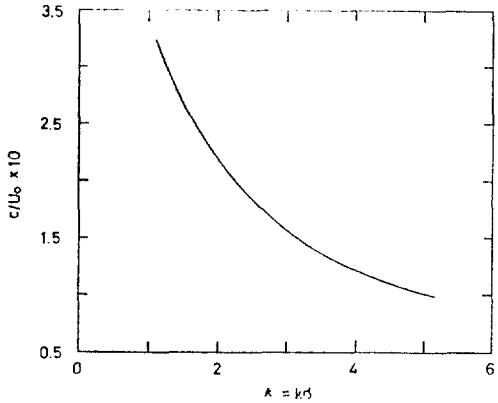

Fig. 5. Phase velocity as a function of wave number.

increases without having any point of inflection, the flow is stable if the upper boundary is rigid in the present problem according to Rayleigh's theorem. However, in our case the upper boundary is free surface and equation (15) seems to give a destabilizing effect.

DISCUSSION

In making a comparison between the measurement and analytical results, U_0 obtained in Table 1 is used while the characteristic boundary layer thickness d is estimated by the following relation.

$$U_0\int_{-\infty}^{0} e^{by}dy=\int_{-d}^{0}\frac{U_0}{d}(y+d)dy$$

which represents the equality of the total momentum represented by U_0e^{by} and the broken line profile. The calculation of d at $x=46$cm gives $d=0.43$cm.

Using $U_0=15$cm/s and $d=0.43$cm, we obtain $f=1.87$ and $\theta=0.4$. In Figure 4 we find that for $\theta=0.4$ the flow becomes unstable when f is smaller than about 0.3, which is much smaller than 1.87 the value obtained above. Thus the shear flow of $U_0=15$cm/s and $d=0.43$cm is stable for all wave number. It can be easily shown that for $d=0.43$cm the flow becomes unstable when U_0 is larger than 37cm/s, which is more than twice the measured surface velocity of $U_0=15$cm/s.

For mathematical simplicity the broken line approximation to shear current was used rather than the exponential form employed in the analysis of experimental results. It may be of interest to try the exponential form. However, the results obtained in the present analysis look reasonable although the analysis is very approximate. One of the general properties of hydrodynamic instability theory of bounded parallel flow is that the phase velocity of the unstable mode is less than the maximum velocity of the undisturbed flow. In Figure 5, $\frac{c}{U_0}<1$ for all κ although in small κ range the curve is not shown. U_0 is the maximum velocity of shear current. Thus the general property is true in the present problem even if the upper boundary is free surface. Therefore, it seems that the wave number associated with wind waves may become unstable in more elaborate calculation. There may exist a great difference between the phase velocity measured and that calculated: the former is about 29cm/s ($\simeq 2U_0$), while the latter can not become larger than U_0.

In conclusion, the instability of shear current seems not to be a possible mechanism of the wind-wave generation even if in a more elaborate calculation the shear current may be unstable hydrodynamically. We can say, however, that the shear current as well as air flow must be taken into account if wind-wave generation is concerned with hydrodynamic instability. The inclusion of air flow may eliminate the phase velocity difference with air velocity being much larger than phase velocity measured. On the other hand Miles' results (1957) shows that the most unstable mode of shear flow is arround $\frac{c}{U_\infty}=0.3$, the ratio of phase velocity to wind velocity, while in our experimental results we find $\frac{c}{U_\infty}=\frac{29}{500}=0.06$ which is clearly means

that the wave motion is not related to the most unstable mode of air flow only.

REFERENCES

Coantic, M. and Favre, A. 1970. Air-sea interaction research program and facilities at I.M.S.T.. 8th symposium on Naval Hydrodynamics. California Institute of Technology, Pasadena. Aug. 23-28.

McLeish, W.L. and Putland, G.E. 1975. The initial water circulation and waves induced by an air flow. NOAA Techn. Report. ERL 316, Boulder, Colorado.

Miles, J.W. 1957. On the generation of surface waves by shear flow. J. Fluid Mech., 3(2):185-204.

Phillips, O.M. 1957. On the Generation of waves by turbulent wind. J. Fluid Mech., 2(5):417-445.

Stern, M.E. and Adam, Y.A. 1973. Capillary waves generated by a shear current in water. Mémoires Société Royale des Sciences de Liège, 6ème série, tome VI, 179-185.